DOI: http://doi.org/10.1016/j.catena.2019.104286

Catena 185 (2020) 104286

Contents lists available at ScienceDirect

Catena

journal homepage: www.elsevier.com/locate/catena

The Late Glacial pedogenesis interrupted by aeolian activity in Central Poland – Records from the Lake Gościąż catchment

Bogusława Kruczkowska[a,*], Mirosław Błaszkiewicz[b], Jerzy Jonczak[a], Łukasz Uzarowicz[a], Piotr Moska[c], Achim Brauer[d], Alicja Bonk[b], Michał Słowiński[e]

[a] Department of Soil Science, Warsaw University of Life Sciences – SGGW, Nowoursynowska Str. 159, 02-776 Warsaw, Poland
[b] Department of Environmental Resources and Geohazards, Polish Academy of Sciences, Institute of Geography and Spatial Organization, Kopernika Str. 9, 87-100 Toruń, Poland
[c] Division of Radioisotopes, Institute of Physics, Centre of Science and Education, Konarskiego Str. 22B, 44-100 Gliwice, Poland
[d] GFZ German Research Centre for Geosciences, Telegrafenberg, 14473 Potsdam, Germany
[e] Department of Environmental Resources and Geohazards, Polish Academy of Sciences, Institute of Geography and Spatial Organization, Twarda Str. 51/55, 00-818 Warsaw, Poland

ARTICLE INFO

Keywords:
Finow soils
Paleosol
The Late Glacial
Pedogenesis
Lake Gościąż

ABSTRACT

An interdisciplinary study was undertaken to reconstruct the Late Glacial fluvioglacial and aeolian sediment transformations with a particular focus on soil-forming processes. The studies included complex pedological research (physical and chemical properties), X-ray diffraction (XRD) analysis of clay minerals and Optically Stimulated Luminescence (OSL) dating on soil/deposit sequences developed within the aeolian landscape of inland dunes in the Lake Gościąż catchment (Central Poland). Late Glacial buried Bwb soil horizons are known as 'Finow soils'. This paleosol was identified in the central part of inland dunes (in vertical perspective), developed from aeolian material deposited on fluvioglacial sediments. The average content of silt and clay in this paleosols ranged from 7.3% to 41.1% and from 6.7% to 12.6%, respectively. In other soil horizons within profiles, the average content of these granulometric fractions was about 3% and 1.5%, respectively. The dominance of dioctahedral vermiculite and the higher content of free iron oxides (especially oxalate form) and aluminium within Bwb horizons indicates their pedogenic origin. The OSL dates suggested that Finow soil fossilization began along with the development of aeolian processes in the late-glacial cold periods (the Older Dryas and the Younger Dryas), while Finow soil development took place in the warmer periods of the Late Glacial (Bølling-Allerød). These results were consistent with data from Germany, other stands in northern Poland and the Tomsk Priobye Region (SE western Siberia).

1. Introduction

Fossil soils (paleosols) are one of the proxies used in environmental reconstructions. Manikowska (1982) and many other researchers reported many stands of fossil soils in central Poland covered with aeolian sediments. It suggests that aeolian sedimentation can create good conditions for preserving the former soil cover. However, the degree of soil profile preservation depends on environmental conditions, particularly during cold periods. Some well-defined groups of paleosols with fully developed profiles or preserved diagnostic horizons with specific features have potential marker character. Examples of such fossil units are Usselo and Finow soils, which, like the Holland Paleosol in North America (Arbogast et al., 2004), are usually considered to be stratigraphic marker horizons for the late-glacial aeolian landscapes in Western and Central Europe (Jankowski, 2012; Kaiser et al., 2009). The term "Finow soil" was used for the first time by Schlaak (1993) to describe the Bwb horizon that commonly occurs in the "Obere Finow" area within the Eberswalde Valley, Germany. Finow soil is an approximately 5–30 cm thick brownish soil without humus horizons and is usually dated from the Allerød age (13.350–12.680 varve years BP) to the beginning of the Younger Dryas (12.680–11.590 varve year BP) (Litt et al., 2001; Litt and Stebich, 1999). These soils are spread within aeolian deposits and inland dunes in the Central European Lowlands creating the so-called "European sand belt" (Koster, 1988; Zeeberg, 1998). This extensive area with dunes and coversands was formed during cold climatic conditions under limited influence of vegetation.

The mechanisms that led to the formation of the Bwb horizon of Finow soils are still not fully understood, but some research indicates a

* Corresponding author.
E-mail address: boguslawa_kruczkowska@sggw.pl (B. Kruczkowska).

https://doi.org/10.1016/j.catena.2019.104286
Received 31 May 2019; Received in revised form 9 August 2019; Accepted 21 September 2019

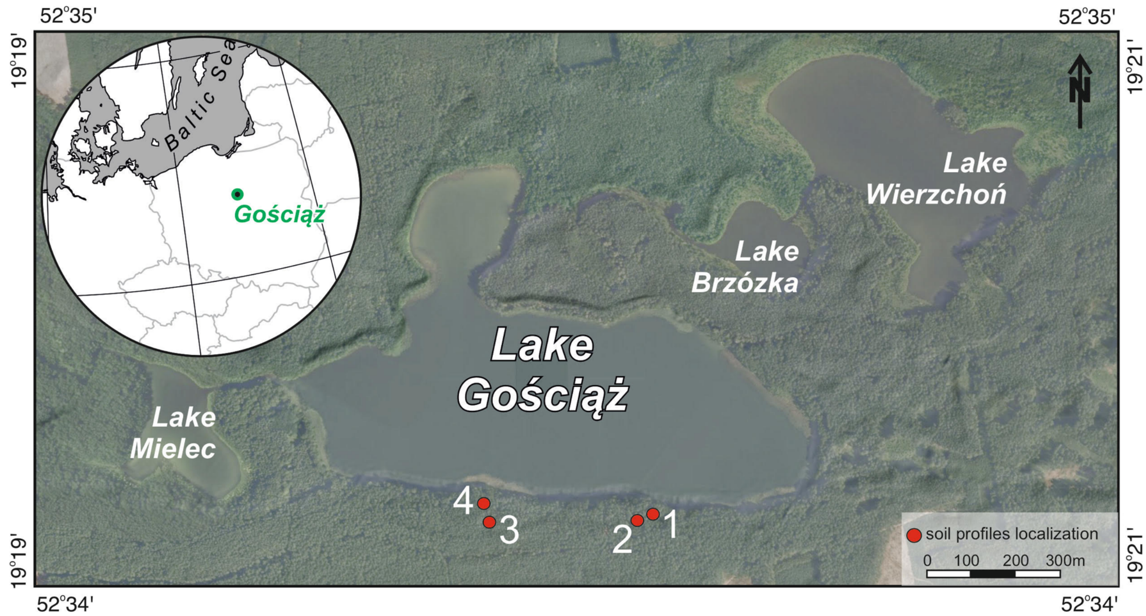

Fig. 1. The localization of the study area.

post-burial process similar to illuvial lamellae formation (Jankowski, 2012). Numerous paleopedological and geomorphological studies on inland dunes of the European sand belt have been conducted (Hirsch et al., 2017; Jankowski, 2002; Jankowski, 2012; Kaiser et al., 2009; Kasse, 2002; Konecka-Betley, 1974; Konecka-Betley, 1981; Konecka-Betley, 1982; Koster, 1988; Kozarski and Nowaczyk, 1991; Manikowska, 1991; Vandenberghe et al., 2013; Zeeberg, 1998). Results of these studies suggest similar stratigraphic position and morphology of fossil soils, related to their coverage by aeolian depositsand development under similar climatic conditions during the Late Glacial. Fossil soil development has been commonly related to climate changes in the Bølling-Allerød interstadial periods when the conditions were warmer and vegetation developed (Ralska-Jasiewiczowa et al., 1998; Słowiński et al., 2017; Zawisza et al., 2019). Soils that developed during the Bølling interstadial are rare and characterized mainly by continuous initial horizons of humus accumulation (Manikowska, 1982), while soils of the Allerød age more often found in Poland than other fossil soils (Jankowski, 2012). Reconstructions of the Allerød mean summer air temperatures conducted on several sites in Poland revealed the temperature varied between 12 °C and 16 °C (Płóciennik et al., 2011; Słowiński et al., 2018; Zawiska et al., 2015). The increase of temperature and air humidity created favourable conditions for vegetation development and surface stabilization (Aichner et al., 2018; Feurdean et al., 2014; Rach et al., 2014; Ralska-Jasiewiczowa et al., 1998). The basic characteristic of plant cover during the Allerød was related to the expansion of forests composed of pine and birch with an increased number of herb and shrub species (Ralska-Jasiewiczowa et al., 1998). Transformations of the natural environment in Europe during the Late Glacial were conditioned primarily by centennial to millennial-scale climatic oscillations from cold stadiums to warm phases, relative environmental stability and vegetation appearance (Brauer et al., 1999; Brauer et al., 2000). These changes influenced the rate and direction of soil development.

The Gościąż Lake is known from its well preserved annually laminated lacustrine sediments that allowed for the reconstruction of environmental changes during the last ca. 14,000 years (Ralska-Jasiewiczowa et al., 1998). Although the detailed environmental reconstructions from Lake Gościąż and its vicinity were carried out in multidisciplinary studies (Ralska-Jasiewiczowa et al., 1998; Sandgren and Thompson, 1990; Wicik, 1998), detailed paleosol investigations have not been performed in this area.

The catchment of Lake Gościąż is occupied by extensive sandy dunes. Contemporary soil cover of inland dunes in Central Poland is not much different. Diversity of soil cover in areas with aeolian sediments depends on the relief of the area and occurrence of local depressions leading to changes in soil moisture. The relief of the area surrounding Lake Gościąż was developed by numerous interacting processes typical of young glacial areas, including accumulation and erosion by glacial meltwater and fluvial activity of the Vistula River, aeolian deflation and accumulation, and dead ice melting processes (Błaszkiewicz et al., 2015; Słowiński et al., 2015). The landscape in the direct vicinity of Lake Gościąż was formed mainly by aeolian processes which led to the formation of sand dunes. Aeolian activity stopped at the beginning of the Holocene when a stable and dense vegetation cover developed in the region (Ralska-Jasiewiczowa et al., 1998). Bølling chronozone was characterized by the occurrence of trees and shrubs which indicate more severe, rather dry and continental conditions (Ralska-Jasiewiczowa et al., 1998). The vegetation recorded during this phase included *Hippophaë*, *Betula pubescens*, *Salix sp.*, *Populus tremula* and open herb vegetation like *Artemisia*, *Chenopodiaceae*, *Helianthemum ssp.*, *Plantago maritima-t.*, *Sedum, Gypsophila fastigiata*. During this period the lake shoreline was occupied by *Typha latifolia*, *Scirpus lacustris -t.*, *Schoenus -t.*, *Equisetum, Sparganium -t.*, *Phragmites* (Ralska-Jasiewiczowa et al., 1998).

Several locations with fossil soils were found in 2018 within the direct vicinity of Lake Gościąż, which gives an opportunity to unravel the processes that lead to the formation of the Bwb horizon of Finow soils. Thus, this paper aims at describing in detail the late-glacial transformation of aeolian sediments including soil-forming and periglacial processes and comparing results with reports of 'Finow soils' in other regions where they were found. An additional objective of the research is also recognition of the physical and chemical properties of the investigated soils.

2. Materials and methods

2.1. Regional settings

Lake Gościąż (52°35́N, 19°21́E) is located within the Vistula Valley between the cities of Płock and Włocławek, Central Poland (Fig. 1), at the bottom of one of the subglacial channels dissecting the surface of a spillway terrace (Churski, 1998). According to the physico-geographical division of Poland (Kondracki, 2001), the study area is located within the Płock Basin mesoregion, which is a part of the Toruń-Eberswalde Glacial Valley macroregion. The lake is a part of the Gostynin-Włocławek Landscape Park, which was established in 1979 to protect the unique nature of this area. Next to the numerous subglacial channels and fluvioglacial terraces, extensive sandy dunes occur in the catchment of Lake Gościąż.

Contemporary soil cover of this area constitutes a mosaic of various soil reference groups strongly affected by origin of parent material, relief and local hydrological conditions. Predominate sandy soils, mostly Brunic Arenosols and Podzols rarely soils developed from glacial till, like Cambisols, Luvisols or Histosols developed from organic sediments (Wicik, 1998).

The lake is surrounded by a forest with *Pinus sylvestris* as the dominant species with an admixture of birch (*Betula pendula*) and oak (*Quercus robur, Quercus petraea)*. Deciduous forests with *Tilia cordata* and *Carpinus betulus*, riverside caars with *Fraxinus excelsior*, *Ulmus minor*, and *Alnus glutinosa*, and alder woods with *Alnus glutinosa*, *Salix cinerea*, *Salix aurita*, and *Salix pentrandra* were also found (Kępczyński and Noryśkiewicz, 1998).

The Płock Basin is characterised by a transitional temperate climate (Woś, 1999). The average annual precipitation for the region is one of the lowest in Poland, amounting to 533 mm/yr (1967–2015) and varying from 340 mm/yr (2015) to 780 mm/yr (2001) (Bartczak et al., 2019). The mean annual precipitation for Płock are maximal in July (82.5 mm) and November (42.00 mm) and minimal in February (25.6 mm) and October (35.7 mm) (Wójcik and Przybylak, 1998). The monthly average air temperatures range from −2.8 °C in January to about 18.1 °C in July (Wójcik and Przybylak, 1998).

2.2. Soil sampling

Four soil profiles with preserved paleosols in the form of Bwb horizons were investigated in this study. All profiles were described according to the FAO standards (FAO, 2006) and classified using the WRB classification system (IUSS Working Group WRB, 2015). Two undisturbed soil samples were collected from every horizon/sedimentary layer using 100 cm^3 steel rings to determine bulk density and porosity. Moreover, one disturbed sample was taken for further analysis. In order to remove rock fragments (> 2 mm), the disturbed samples were dried at 40 °C and sieved through a 2.0 mm sieve. Additionally, a large amount of humus was collected for plant macrofossils analysis and prepared with a standard procedure (Birks, 2007).

2.3. Analysis of soil's physical and chemical properties

Particle size distribution of the soils was determined using the combined method of pipette and sieve. Grain fractions and soil textural classes were identified according to the Polish Soil Science Society (Polskie Towarzystwo Gleboznawcze, 2009), which is consistent with United States Department of Agriculture (USDA) classification (USDA, 1993). Next, we calculated geometric graphical measures after Folk and Ward (1957), including mean diameter (MG), sorting (σG), skewness (SkG), and kurtosis (KG), using GRADISTAT 5.11 software (Blott and Pye, 2001). The reaction (pH) was measured potentiometrically in a suspension with deionized water and 1 mol·dm^{-3} KCl in the soil: water/KCl ratio of 1:2.5 (pH-meter Elmetron CPC-401). Bulk density and total porosity were established for undisturbed soil samples by using the drying-weight (gravimetric) method. Total organic carbon (TOC) was determined using a TOC analyser (Shimadzu 5000A), total nitrogen (TN) with the Kjeldahl method (van Reeuwijk, 2002). Total content of elements was determined in a solution after digestion of samples in a mixture of 40% HF and 60% $HClO_4$ using a high-pressure microwave digestion system (Milestone EthosPlus). The P content in a solution was analysed by means of the molybdenum blue method (van Reeuwijk, 2002), whereas concentrations of K, Ca, Mg, Fe, Al, and Mn were determined by flame atomic absorption spectrometry (Perkin Elmer AAS 2100). "Free" iron oxides (Fe_d) were extracted by Mehra and Jackson's (1960) procedure, whereas amorphous and poorly-crystalline iron (Fe_o) and aluminium (Al_o) oxides by Schwertmann's procedure (van Reeuwijk, 2002). Based on these results, Fe_d/Fe_t (weathering ratio) and Fe_o/Fe_d ratio were calculated.

2.4. OSL-dating

Nine samples for the Optically Stimulated Luminescence (OSL) dating were collected from C horizons located at different depths from three profiles (1, 3, and 4) above and below paleosols. Steel tubes were used during sampling to protect sediment from sunlight. In the OSL Laboratory in Gliwice, Poland samples were opened, dried, and prepared both for gamma spectrometry and luminescence measurements under dark conditions. High-resolution gamma spectrometry was used in order to determine U, Th, and K contents in the samples by means of a HPGe detector (Canberra). Each measurement lasted for at least 24 h. Prior to measurement, the samples were stored for about three weeks to ensure equilibrium between gaseous ^{222}Rn and ^{226}Ra in the ^{238}U decay chain. The activities of the isotopes were determined using IAEA standards RGU, RGTh, RGK after subtracting the detector background. Using (Guerin et al., 2011) conversion factors, dose rates were calculated. Prescott and Stephan (1982) procedure was used for the cosmic ray beta dose-rate calculation.

We assumed that the samples' average water content for most of the time was 5 ± 2%, since this humidity is typical for sandy sediments. The humidity was set to this level because we have not been able to precisely reproduce changes in this type of sediment for the last several thousand years. Changes of environmental conditions, mainly climatic, may lead to the transformation of humidity levels of soils, so the water content during sampling should not be treated as the correct value for total burial span (Rosenzweig and Porat, 2015). Duller (2008) noticed that 1% of water content would contribute 1% underestimation of the OSL age.

Using standard purification procedures (e.g. Aitken (1998), sand-sized grains of quartz (90–200 μm in diameter) were extracted from the sample. The quartz grains were separated using density separation with the application of sodium polytungstate solutions leaving grains of densities between 2.62 g cm^{-3} and 2.75 g cm^{-3}. Finally, the quartz grains were etched in 40% hydrofluoric acid for 60 min to remove the outer 10 mm layer, which absorbed a dose of alpha radiation (Aitken, 1998).

All OSL measurements were made by means of an automated Risø TL/OSL DA-20 reader using multi-grain aliquots, each of approximately 1 mg. The stimulation light source was a blue (470 ± 30 nm) light emitting diode array delivering 50 mW cm^{-2} at the sample (Bøtter-Jensen et al., 2000). Detection was through 7.5 mm of Hoya U-340 filter. Using the single-aliquot regenerative-dose protocol (Murray and Wintle, 2000), equivalent doses were determined. The Central Age Model (Galbraith et al., 1999) was used to determine the luminescence ages.

2.5. XRD analysis of clay fraction

The clay fractions were separated from selected fossil Bwb horizons by means of Jackson (1975) procedure. Carbonates were removed using an acetic acid buffer (pH ~ 5). Organic matter was removed using 30% hydrogen peroxide buffered with an acetic acid buffer (pH ~ 5). Free Fe oxides were removed using sodium dithionite buffered with a citrate-bicarbonate solution according to Mehra and Jackson (1960) method. Clay fractions (< 2 μm) were separated by centrifugation. Aliquots of clay fractions were saturated with Mg and K and dialyzed. Oriented mounts on glass slides were prepared by sedimentation. They were analysed using XRD method by means of the Bruker AXS D5005 diffractometer equipped with the KRISTALLOFLEX® 760 X-ray generator, the vertical goniometer, 1 mm divergence slit, 2 mm anti-scatter slit, 0.6 mm detector slit, and a graphite diffracted-beam monochromator. CoKα radiation was used by applying a voltage of 40 kV and 30 mA current. Oriented mounts were scanned at a counting time of 2 s per 0.02° step from 3 to 40 °2θ. The XRD analyses were performed in air-dry conditions (Mg- and K-saturated samples), after ethylene glycol (EG) treatment (Mg-saturated samples only), and after heating for at least 1 h at 330 °C and 550 °C (K-saturated samples only).

In order to determine if clay minerals are di- or trioctahedral, XRD analyses of random powder mounts from clay fractions were performed in the d_{060} range (from 68 to 76° 2θ CoKα at counting time of 2 s per 0.005° step and the applied voltage of 40 kV and 35 mA current).

3. Results

3.1. Morphology and classification of the soils

The studied profiles were located on the top or slope of dunes and are represented by dry and poorly developed soils, including Dystric Brunic Arenosols (Aeolic, Protospodic) and Dystric Brunic Arenosols (Aeolic) with moderately marked B horizons (IUSS Working Group WRB, 2015) (Fig. 2).

In profiles 1 and 2 secondary podzolization process was observed resulting in the formation of Bohs horizons in the topsoil. Parent material of these soils constituted fine aeolian sand. Paleosols located at the depths of 120 cm and 163 cm from profile 1 and 2, respectively, were composed of brownish 10–30 cm thick Bwb horizons without buried humus horizons and were classified as Eutric Brunic Arenosols (Relictiturbic) (Fig. 2). Similar horizons at the depth of 110 cm and 120 cm in profiles 3 and 4 were classified as Eutric Cambisols (Loamic) (IUSS Working Group WRB, 2015). Differences in Bwb horizons classification were caused by their texture. In profiles 3 and 4, high content of silt and clay (up to 41.1% of silt and to 14.0% of clay) was determined to be what classifies these profiles as Cambisols. Intermixing of fossil humus horizons into the lower B horizons by cryoturbation was not observed in studied profiles. Evidences of cryoturbation in a form of about 10–20 cm thick ice wedges within 3Bw@b horizon in profile 1 and 2Bw@b horizon in profile 2 were found. In profile 2, 10-cm thick ice wedges were visible on the side walls of the soil pit. In all profiles, thin, horizontally stratified illuvial lamellae occur below Bwb horizons. The top and bottom transitions between Bwb and neighbouring horizons were mostly gradual (profile 1 and 2), however, there was a lack of finger-like protuberances between these brownish horizons and other deposits. Transition below Bwb horizons was sharp in profile 3 and 4.

3.2. Physical properties of the soils

Particle density of the soils related to quartz characteristics and reached values ranging from 2.51 g cm^{-3} to 2.59 g cm^{-3} in A, AEs, and ABo horizons to 2.51 g cm^{-3} –2.66 g cm^{-3} in sandy substrate and in Bw/C horizons (Fig. 3). These values ranged from 2.51 g cm^{-3} to 2.62 g cm^{-3} in Bwb horizons. Bulk density in profiles 1–3 increased with the depth from 1.28 g cm^{-3} to 1.34 g cm^{-3} in humus horizons and from 1.04 g cm^{-3} to 1.63 g cm^{-3} in mineral horizons (excluding Bwb horizons). In profile 4, characterized by mixed material in topsoil (the result of natural slope processes), the diversification of bulk density values from 1.36 g cm^{-3} –1.45 g cm^{-3} in surface horizons to 1.65 g cm^{-3} in other mineral horizons) was observed. The bulk density of fossil Bwb horizons also varied, reaching values from 1.07 g cm^{-3} to 1.66 g cm^{-3}.

Total porosity in profiles 1–3 decreased with depth (including paleosols), reaching the highest values (up to 49.3%) in humus horizons (Fig. 3). Bwb horizon in profile 3 had clearly increased porosity (up to 58.5% in 4Bwb and 60.2% in 4Bw/5Cb horizon) in comparison to neighbouring horizons. Omitting the increased porosity in profile 3 the average porosity of fossil Bwb horizons is 38.7%.

The youngest soils located on the top of the profiles (Dystric Brunic Arenosols) had brownish-black or dark brown humus horizons, brown or yellowish-brown Bo horizons, and dull yellow-orange or bright yellowish-brown parent material (Fig. 3). In contrary to contemporary soils at the study area, fossil brown Bwb horizons (Finow soils) in profiles 1, 2 and 4 reached colours from the hue of 7.5YR. Dull yellow-orange and yellowish-brown (hue 10YR) Bwb horizons occur in profile 3 (Fig. 3).

3.3. Chemical properties of the soils

The youngest soils – Dystric Brunic Arenosols (Aeolic, Protospodic) in profile 1 and 2 and Dystric Brunic Arenosols (Aeolic) in profile 3 and 4 – are characterized by a lack of $CaCO_3$ and had extremely acidic (in A and B horizons) to strongly acidic (in parent material) soil reaction (Table 1). However, C1 and C2 horizons in profile 2 had slightly acidic to neutral soil reaction (Table 1). Increased content of $CaCO_3$ was observed in the subsoil of profiles 2, 3 and 4, which caused the increase of soil pH up to 8.41 in 5C2b (profile 4). The highest content of $CaCO_3$ (12%) was measured in 4Bwkb horizon in profile 4. Reaction of fossil Bwb horizons was diverse, from strongly acidic (profile 3) to neutral (profile 4) (Table 1).

TOC and TN contents were generally low (BK5, 2005) and reached maximum values in humus horizons (3.55–19.64 g kg^{-1} and 0.32–1.21 g kg^{-1}, respectively) (Table 1). In all studied Dystric Brunic Arenosol profiles (in the topsoil of all studied profiles), TOC and TN content decreased with the depth. Compared to the sandy material of other horizons, a slight increase in the content of these elements was noticeable in brownish Bwb horizons, which may indicate the existence of a plant cover on these soils in the past. The 4Bwkb horizon (profile 4) was characterized by the TOC content increasing to 12.87 g kg^{-1} and low content of TN (0.14 g kg^{-1}). Bwb horizons usually contain more TOC than adjacent horizons, which also means that they probably were developed on the surface under vegetation cover. Values of C/N ratio in humus horizons ranged from 10.9 to 18.8, while these values were lower with a maximum of 17.7 in Bo and C horizons of young Dystric Brunic Arenosols. The increase of these indicator values was also observed in Bwb horizons (4.6–92.2).

P, K, Ca and Mg content in sandy horizons was low (Table 2). The phosphorus content in the studied profiles ranged from 0.20 g kg^{-1} to 0.47 g kg^{-1} in topsoil and from 0.11 g kg^{-1} to 0.57 g kg^{-1} in sandy horizons, with a general increasing trend downwards the profile. A similar regularity also concerned magnesium. Its content varied from 0.28 g kg^{-1} to 0.59 g kg^{-1} in A horizons and from 0.30 g kg^{-1} to 0.98 g kg^{-1} in the other horizons. The potassium content was strongly conditioned by the origin of soil mineral substrates and reaching values of 7.01–12.63 g kg^{-1} in all sandy horizons, and 11.95–15.17 g kg^{-1} in Bwb horizons. The investigated soils were poor in calcium in general. However, increased content of this element was observed in Bwb horizons.

Sorption complex of the studied soils varied among profiles and horizons, including capacity and saturation with various ionic components. Topsoils of Dystric Brunic Arenosols (profiles 1–4) were characterized by low base saturation (5.2–19.2%), which increased to 96.7% in most of BoC and C horizons (excluding profile 3) (Arbeitskreis Standortskartierung, 1996). Fossil soils were saturated with bases in more than 90%, except for 4Bwb horizon in profile 3, where it was only 6.5% (Table 2). Profile 3 had the lowest base saturation among all profiles with the mean value not exceeding 10.1% for most of the horizons.

3.4. Characteristics of iron and aluminium forms

The Fe_t content in sandy horizons of Dystric Brunic Arenosols (topsoil of profiles 1–4) was similar within the profiles. These values were low and ranged from 2.36 g kg^{-1} to 4.95 g kg^{-1} (Fig. 4). In Bo

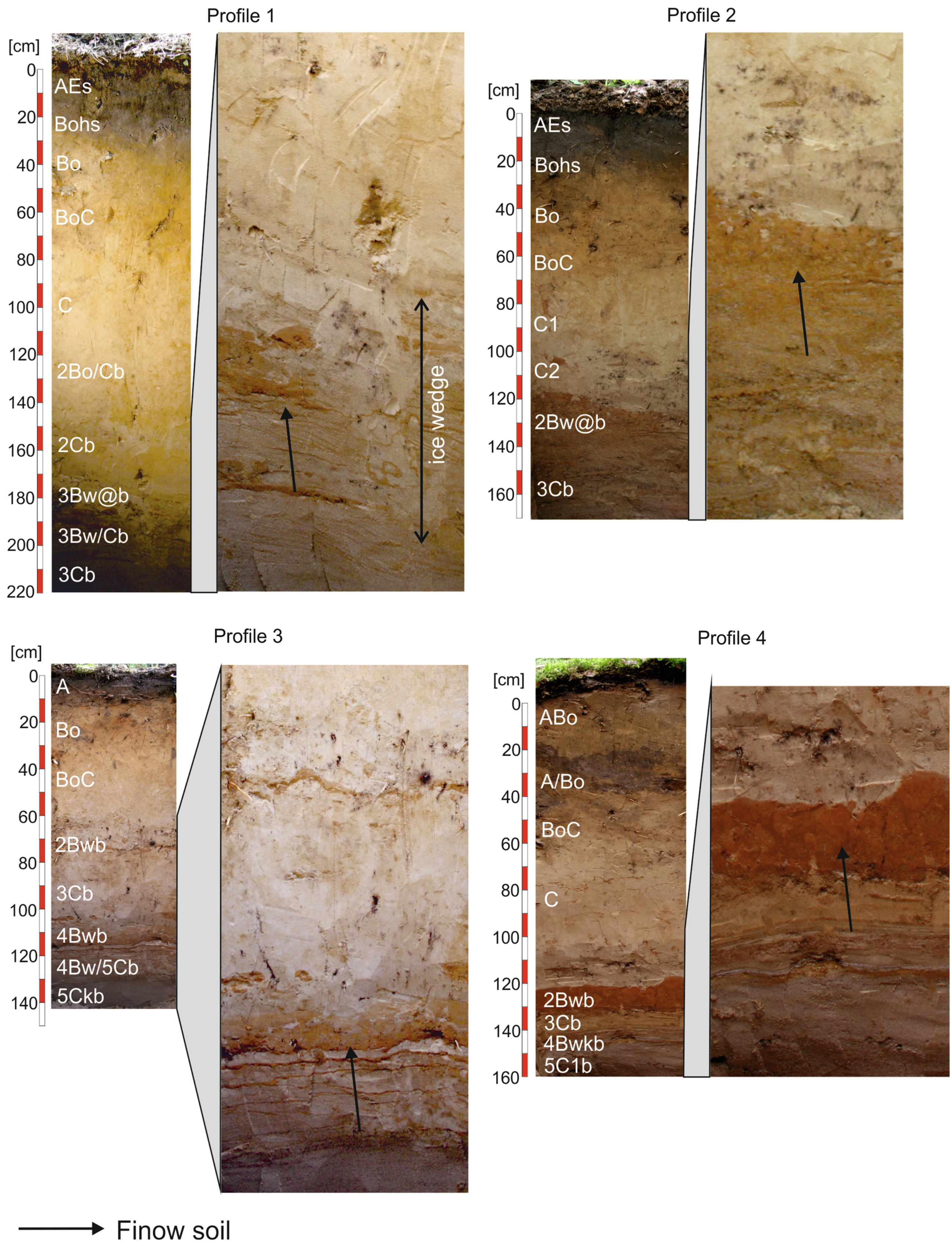

Fig. 2. Studied soil profiles.

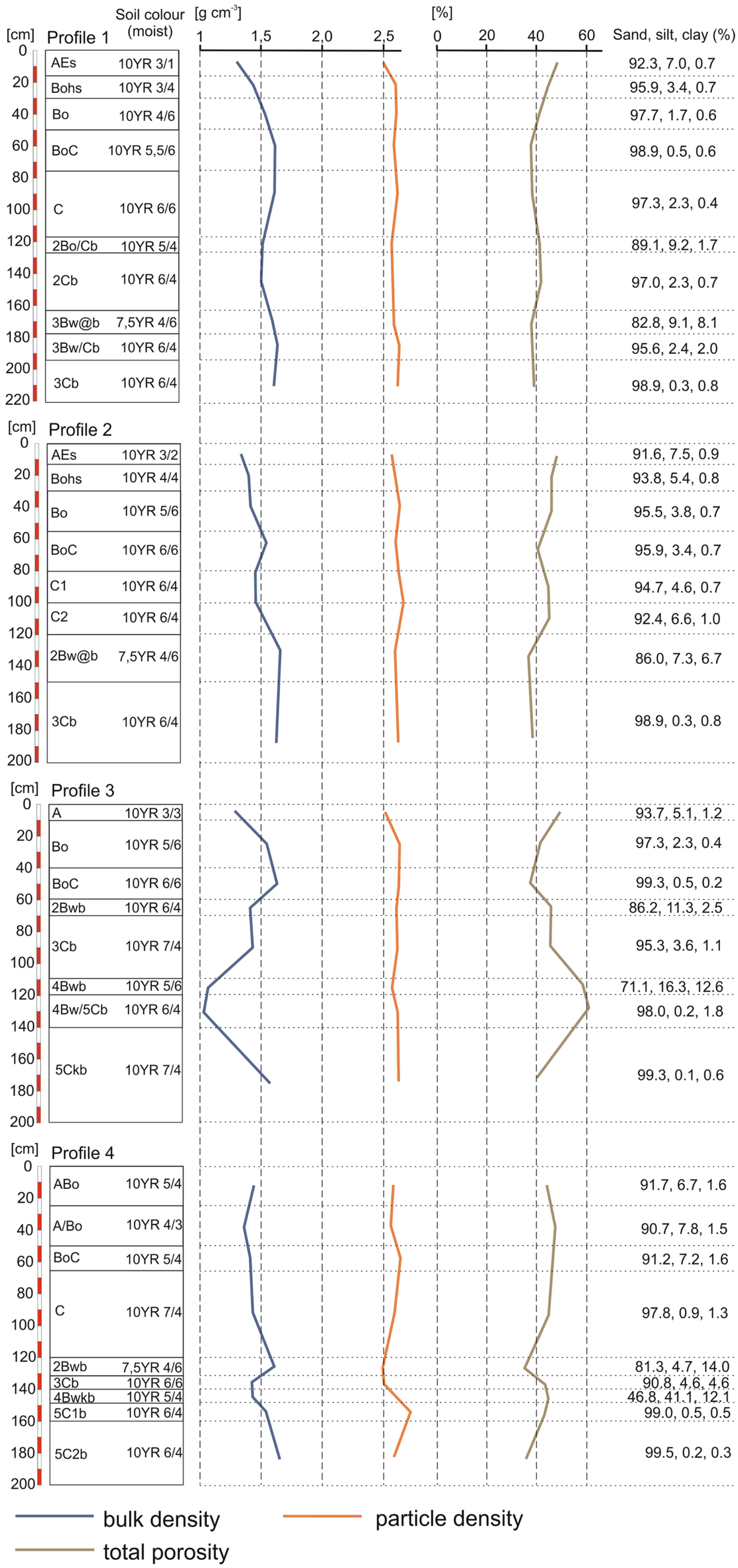

(caption on next page)

Fig. 3. Selected physical properties of the soil profiles.

Table 1
Selected chemical properties of the studied soils.

Depth [cm]	Soil horizon	pH-H_2O	pH-KCl	$CaCO_3$ [%]	TOC [g kg^{-1}]	TN [g kg^{-1}]	TOC:TN
Profile 1							
0–15	AEs	4.05	3.00	0.0	19.64	1.24	15.9
15–30	Bohs	4.23	3.56	0.0	6.54	0.46	14.1
30–50	Bo	4.41	3.88	0.0	2.64	0.20	13.2
50–75	BoC	4.77	4.09	0.0	0.37	0.05	6.8
75–117	C	5.14	4.41	0.0	0.00	0.05	–
117–127	2Bo/Cb	4.38	3.57	0.0	1.84	0.11	16.1
127–163	2Cb	5.00	4.07	0.0	0.00	0.04	–
163–177	3Bw@b	5.40	4.61	0.0	0.35	0.08	4.6
177–193	3Bw/Cb	5.60	4.75	0.0	0.00	0.03	–
193–220	3Cb	5.66	4.85	0.0	0.00	0.02	–
Profile 2							
0–13	AEs	4.38	3.18	0.0	12.58	0.91	13.8
13–30	Bohs	4.58	3.51	0.0	7.41	0.45	16.5
30–55	Bo	5.11	3.77	0.0	3.18	0.22	14.2
55–80	BoC	5.86	4.01	0.0	0.70	0.08	9.3
80–100	C1	6.37	4.41	0.0	0.00	0.05	–
100–120	C2	6.64	4.75	0.0	0.00	0.07	–
120–150	2Bw@b	6.28	4.45	0.0	0.79	0.13	6.0
150–200	3Cb	6.09	5.62	0.4	0.00	0.03	–
Profile 3							
0–10	A	4.16	3.26	0.0	10.60	0.56	18.8
10–40	Bo	4.21	3.94	0.0	3.66	0.21	17.7
40–60	BoC	4.74	4.17	0.0	0.27	0.05	6.0
60–65	2Bwb	5.41	4.54	0.0	0.00	0.04	–
65–110	3Cb	5.00	3.96	0.0	0.00	0.03	–
110–120	4Bwb	3.51	2.85	0.0	1.24	0.11	11.1
120–140	4Bw/5Cb	3.93	3.60	0.0	0.00	0.02	–
140–200	5Ckb	6.35	5.22	2.9	0.00	0.01	–
Profile 4							
0–25	ABo	4.38	3.62	0.0	3.55	0.32	10.9
25–50	A/Bo	4.43	3.82	0.0	4.92	0.37	13.3
50–65	BoC	4.76	3.94	0.0	2.07	0.16	13.0
65–120	C	5.26	4.77	0.0	0.00	0.03	–
120–132	2Bwb	5.46	4.41	0.0	0.69	0.12	5.8
132–140	3Cb	5.72	5.54	0.0	0.00	0.04	–
140–148	4Bwkb	6.95	6.75	12.0	12.87	0.14	92.2
148–160	5C1b	8.23	7.51	2.6	0.00	0.02	–
160–200	5C2b	8.41	7.75	3.2	0.00	0.01	–

horizons, a small increase of about 0.2–0.5 g kg^{-1} was observed. In fossil Bw horizons, a considerable increase of Fe_t content (up to 13.09 g kg^{-1}) was recorded. Among the forms of this element, the so-called free iron oxides (Fe_d) clearly predominated, constituting 13–50% of Fe_t. Fe_d/Fe_t ratio varied in the studied profiles, reflecting the effect of soil-forming processes. Crystalline iron forms predominated over amorphous forms in general, which is reflected in Fe_o/Fe_d ratios (Fig. 4). In some horizons of the contemporary soils, the predominance of amorphous forms was observed.

The total content of Al_t in the studied soils was higher than Fe content and ranged from 10.37 g kg^{-1} to 31.52 g kg^{-1} (Fig. 4). When compared to the contemporary soils in topsoil, the highest contents of Al_t occurred in fossil Bwb horizons. Increased content of Al_t is also observed within other B horizons. However, these values were lower than in Bwb and reached a maximum of 20.14 g kg^{-1}. In contrast to the Fe_t, the Fe_o content was the highest to a depth of about 60 cm and ranged from 0.51 g kg^{-1} to 1.69 g kg^{-1}. Within fossil Bwb horizons Fe_o content was about 0.23 g kg^{-1}–1.25 g kg^{-1}. Average amount of Al_o in Al_t was about 6% (values from 0.03 g kg^{-1} to 1.69 g kg^{-1}). The value of the Al_o/Al_t ratio decreased with depth and ranged from 0.3 to 0.14 in surface horizons to 0.00–0.02 in the lower parts of the profiles. Only in Bwb horizon in profile 3 this value was higher than in neighbouring horizons, reaching a value of 0.04.

3.5. OSL age, origin, and textural parameters of deposits

According to the results of OSL dating, the last phase of glaciofluvial sand deposition in the studied area took place between 13.32 ± 0.80 ka (GdTL-2843) and 13.71 ± 0.66 ka (GdTL-2846) (Table 3). Sandy aeolian deposits covering Bwb horizons were dated to 11.28 ± 0.59–13.86 ± 0.70 ka (GdTL- 2842 and GdTL-2848). An inversion of dates was observed in profile 1.

Every top and bottom part of the investigated profiles was developed from loose, moderately- or poorly-sorted glaciofluvial sands remodelled by aeolian processes with mainly symmetrical or positively skewed particle-size distribution curves. The particle-size distribution reveals a homogenous sediment unit of fine sand, sand, and loamy sand. However, Bwb horizons developed from very poorly sorted sandy loam, loam, and silty loam deposits with positively skewed, strongly positively skewed, or negatively skewed particle size distribution curves. The dominant fractions of 0.5–0.25, 0.25–0.1, and 0.1–0.05 mm constituted in total about 90–97% of the sandy horizons. An increased content of silt (7–52%) and clay (7–23%) was observed in buried Bwb horizons (Fig. 3), whereas in other horizons these values vary from 0.2% to 9.3% for silt content and to 1.6% for clay.

Mean grain size in each profile varied from 0.15 mm to 0.17 mm. Lower values occurred only in the zone from 2Bwb to 4Bwb horizons in profile 3 (0.09 mm) and in 2Bwb to 4Bwkb horizons in profile 4

Table 2
The total content of P, K, Ca, and Mg and base saturation of the studied soils.

Depth [cm]	Soil horizon	P [g kg^{-1}]	K [g kg^{-1}]	Ca [g kg^{-1}]	Mg [g kg^{-1}]	BS [%]
Profile 1						
0–15	AEs	0.40	9.04	1.61	0.35	19.2
15–30	Bohs	0.57	9.37	4.45	0.38	13.0
30–50	Bo	0.57	9.03	2.20	0.54	15.2
50–75	BoC	0.30	9.15	2.59	0.48	28.9
75–117	C	0.27	10.70	2.92	0.61	80.8
117–127	2Bo/Cb	0.21	11.39	2.45	0.98	5.6
127–163	2Cb	0.22	12.12	3.07	0.72	56.4
163–177	3Bw@b	0.30	11.95	3.00	1.69	98.7
177–193	3Bw/Cb	0.21	9.03	2.80	0.69	95.7
193–220	3Cb	0.21	8.31	2.46	0.47	96.3
Profile 2						
0–13	AEs	0.47	10.47	1.57	0.44	11.1
13–30	Bohs	0.56	10.77	1.84	0.56	13.0
30–55	Bo	0.55	11.13	1.17	0.47	13.4
55–80	BoC	0.36	11.87	2.70	0.72	50.1
80–100	C1	0.26	12.63	2.72	0.77	85.5
100–120	C2	0.22	11.56	3.12	0.80	96.7
120–150	2Bw@b	0.39	12.61	4.46	2.83	98.0
150–200	3Cb	0.29	7.48	5.07	0.48	99.6
Profile 3						
0–10	A	0.20	8.93	1.05	0.28	5.2
10–40	Bo	0.50	9.03	0.93	0.30	6.5
40–60	BoC	0.20	8.99	1.85	0.41	14.1
60–65	2Bwb	0.21	14.19	2.75	1.10	94.5
65–110	3Cb	0.11	13.03	2.01	0.67	14.4
110–120	4Bwb	0.23	14.89	2.54	2.77	6.5
120–140	4Bw/5Cb	0.13	9.30	2.46	0.71	14.1
140–200	5Ckb	0.26	7.01	21.78	0.79	100.0
Profile 4						
0–25	ABo	0.26	10.71	2.71	0.59	8.9
25–50	A/Bo	0.22	10.86	1.77	0.51	17.2
50–65	BoC	0.27	11.17	1.50	0.62	31.9
65–120	C	0.21	12.26	2.47	0.60	90.9
120–132	2Bwb	0.41	13.86	4.80	2.45	98.1
132–140	3Cb	0.32	13.32	4.35	1.34	98.6
140–148	4Bwkb	0.62	15.17	84.23	7.84	99.7
148–160	5C1b	0.27	8.60	21.68	1.02	100.0
160–200	5C2b	0.21	7.71	25.60	0.85	100.0

(0.06 mm; Fig. 5). A considerable increase in average grain size was recorded in bottom horizons (from 0.21 mm to 0.49 mm) of all profiles. Bwb horizons from profiles 1 and 2 were characterized by a larger admixture of coarser fractions. Bwb horizons with best-developed morphology occurred in profile 3 and 4. They were characterized by a distinct mean grain size reduction to 0.03 mm and 0.04 mm, respectively (Fig. 5).

The macrofossil analysis showed that there was a lack of fossils in analyzed samples.

3.6. Mineral composition of clay fractions from fossil Bwb horizons

Mineral composition of clay fractions was similar in each fossil Bwb horizon in this study (Fig. 6). Swelling phases were represented by vermiculite (the d_{001} peak at 1.42 nm when saturated with Mg^{2+} both in air-dry state and after EG solvation; the peak disappears after heating), smectite (the d_{001} peak at ≈1.68 nm when saturated with Mg^{2+} after EG treatment; the peak disappears after heating), and certain mixed-layer minerals containing swelling layers (most likely of illite-smectite type) (Fig. 6). Non-swelling phases identified in all investigated Bwb horizons are illite (the d_{001} peak at ~1.0 nm that does not change its position, neither after EG treatment nor after heating) and kaolinite (the d_{001} and d_{002} peaks 0.717 nm and 0.357 nm, respectively, that do not shift after EG treatment and heating at 330 °C, but disappear after heating at 550 °C). Apart from these minerals, clay fractions from soils also contained admixtures of quartz and feldspars (orthoclase and albite). Clay fraction from 4Bwkb horizon (140–148 cm) in profile 4 most likely contained traces of some zeolite (heulandite and/or clinoptilolite), indicated by the presence of weak 0.898 nm peak in the XRD pattern of the sample.

The analysis of XRD patterns of the random powder mounts from clay fractions (Fig. 7) revealed the presence of the broad peak 0.149–0.151 nm, indicating that clay minerals (i.e., illite, kaolinite, vermiculite, and smectite) in B horizons are dioctahedral species. The peak 0.154 nm can belong to quartz or trioctahedral clay minerals. This sharp peak indicated that it belongs rather to quartz than trioctahedral clays (the peak for clays is typically a broad one).

4. Discussion

4.1. Age of Finow soils

A compilation of ages obtained from Usselo and Finow soils in Central Europe (Germany and Poland) revealed the main time range for soil formation between the Older Dryas and the Younger Dryas with single examples developed in the Preboreal period (Kaiser et al., 2009). However, according to (Schlaak and Kowalski, 2015), the beginning of these soils' development can be related to the Bølling interstadial. For most of the paleosols described in Poland, similar ages were reported. In contrast, the older Late Glacial paleosols represented by initial Gleysols were reported rarely. Some examples were known from the Kamion/Epe interstadial – a warm period before the Oldest Dryas (Kolstrup, 1980; Manikowska, 1970; Manikowska, 1991) and the Bølling interstadial (Konecka-Betley, 1991; Krajewski and Balwierz, 1984). OSL-dating of aeolian deposits covering the studied fossil soils showed that those deposits developed in the older part of the Late Glacial in warm periods: the Meinendorf interstadial (between 14.450 and 13.800 varve years BP) and the Bølling (13.670–13.540 varve years BP; (Litt et al., 2001; Litt and Stebich, 1999)). It is possible that the soil-formation phase of the Finow soils was recorded in all analysed profiles from Lake Gościąż vicinity. Hence, the commonly assumed formation of the paleosols in the Allerød interstadial cannot be confirmed by geochronological data alone and it is thus more appropriate to consider these soils more generally as of the Late Glacial age (Kaiser et al., 2009).

OSL dating from profiles 3 and 4 revealed statistically indistinguishable ages (based on chi-squared test): a sample from aeolian sediments above the Finow soil in profile 3 dated at 13.53 ± 0.74 ka (GdTL-2845), a sample above the soil in profile 4 dated at 14.36 ± 0.84 (GdTL-2847), and a sample below the soil in profile 4 dated at 13.86 ± 0.70 ka (GdTL-2848). These results were in agreement with published ages of 13.5 ka in Mecklenburg, NE Germany, and of 13.3 ± 1.2 ka in NE Estonia (Kalińska-Nartiša et al., 2015) suggesting that this age range generally marks the time of burial of these soils (Küster et al., 2014; Küster and Preusser, 2009). This age range was also reported from recent research of Finow soils in the Tomsk Priobye Region, SE Western Siberia (Konstantinov et al., 2019). Inversion of dates in profile 1 was related to the high variability of radioisotopes content, which translated into a dose rate change of about 50% in an area of just over ten centimetres. Such changes suggest that materials with different physical and chemical properties have been deposited. According to the OSL age of the studied samples, the estimation and assumption was made that aeolian activity mainly occurred during cold periods of the Late Glacial. The beginning of aeolian processes led to the formation of dunes in the Płock Basin probably started during the Oldest (13.800–13.670 varve years BP) and the Older Dryas (13.540–13.350 varve years BP; (Litt et al., 2001; Litt and Stebich, 1999)). Since these ages were also obtained from aeolian sediments covering the soil, we must assume that soil formation took place before the Allerød. A pre-Allerød age of aeolian processes in the direct vicinity of Lake Gościąż was further suggested by geomorphological relations between large dune forms and subglacial channels. Generally, in cases of their direct contact, the dune forms distinct "cut" at the edges of

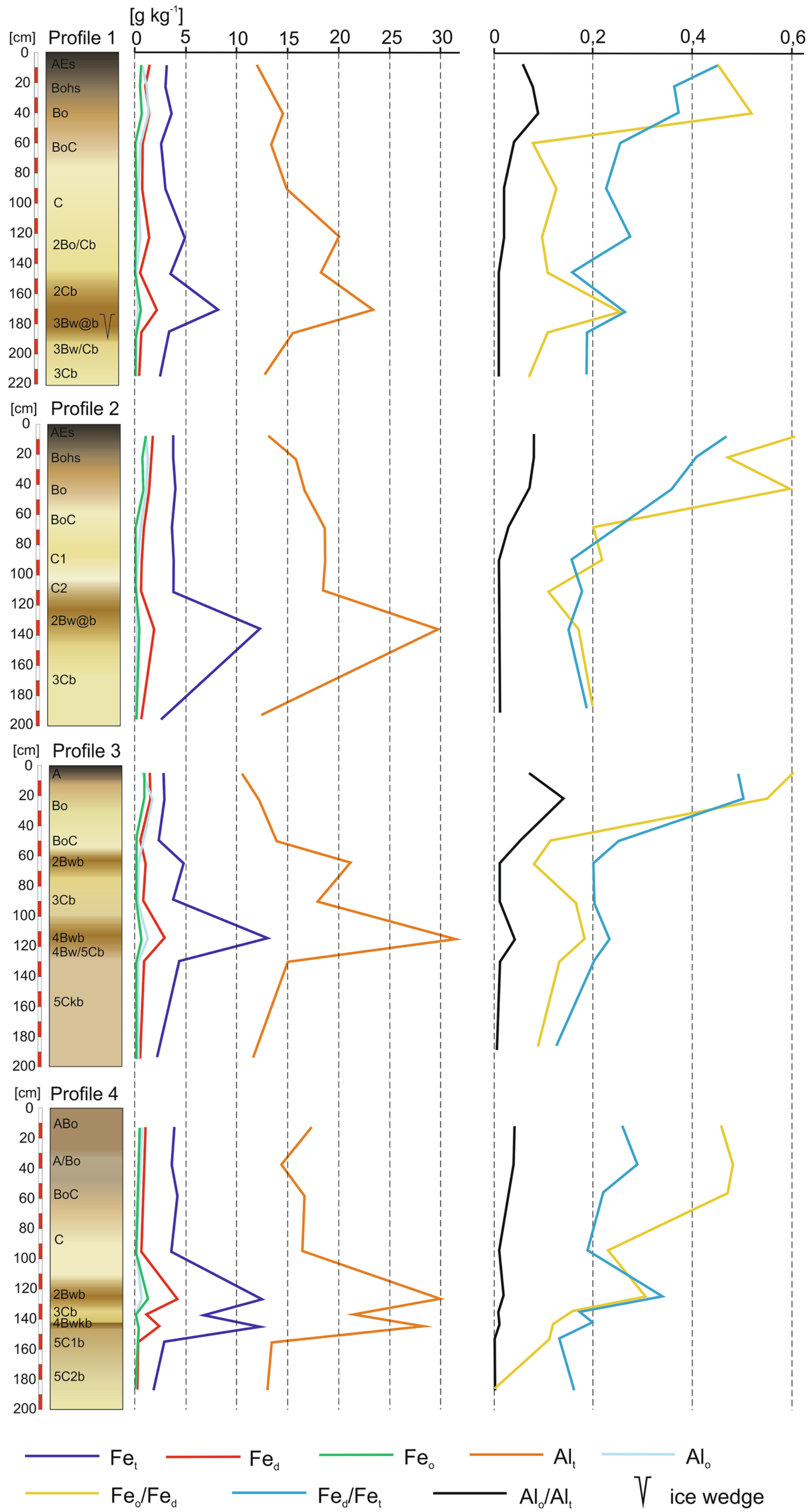

Fig. 4. Content of Fe and Al forms in the studied soil profiles.

Table 3
OSL-age of selected soil samples collected from horizons located below and above Bwb horizons.

Profile	Sample	Soil horizon	Depth (cm)	Dose rate (Gy/ka)	OSL age (ka)
1	GdTL-2840	C	100	1.43 ± 0.06	12.86 ± 0.73
1	GdTL-2841	2Bo/Cb	120	2.10 ± 0.09	11.50 ± 0.59
1	GdTL-2842	2Cb	150	2.15 ± 0.08	11.28 ± 0.59
1	GdTL-2843	3Cb	200	1.22 ± 0.05	13.32 ± 0.80
3	GdTL-2844	BoC	50	1.44 ± 0.06	13.02 ± 0.80
3	GdTL-2845	3Cb	80	1.94 ± 0.08	13.53 ± 0.74
3	GdTL-2846	3Ckb	150	1.64 ± 0.05	13.71 ± 0.66
4	GdTL-2847	C	100	1.78 ± 0.08	14.36 ± 0.84
4	GdTL-2848	3Cb	135	2.09 ± 0.08	13.86 ± 0.70

subglacial channels is what indicates the accumulation of dunes before the final stage of dead ice melting and preserving subglacial channels. The sediment cores from the deep basin of Lake Gościąż showed that the beginning of dead ice melting in this region began in Bølling (Błaszkiewicz, 2011; Błaszkiewicz and Gruszka, 2005; Ralska-Jasiewiczowa et al., 1998), while the final melting of buried blocks of dead ice occurred in the late Allerød. However, OSL dates of deposits above the Bwb horizon in profile 1 revealed a younger age of 11.28 ± 0.59 ka (GdTL-2842), which would allow for dating the soil formation to the Allerød. These discrepancies in OSL-dating of Finow soils from Germany and Poland may result from local variability of soil water content. Soil moisture of 5 ± 2% was used to obtain the majority of OSL-dating results of sediments neighbouring to Finow soils; assuming that this value is the long-term average, it is the most optimal for sandy sediments. The remodelling of the previously formed dunes and new dune formation processes most likely took place in the Younger Dryas (Rychel et al., 2018). In the neighbouring Toruń Basin located about 50 km northwest from the research area, the main dune-formation phase was dated to the Younger Dryas (Jankowski, 2012). This is in agreement with the result from our profile 1 but disagrees with our profiles 3 and 4. These differences may be explained by OSL dating problems or may indicate that aeolian processes were active during the entire Late Glacial (Table 3) but with large spatial diversity and local differences. Despite the remaining uncertainties in absolute dating of the pedogenic processes and the similarity of ages below and above the paleosols, the results indicated that the Bwb horizons may have developed in a relatively short time. The OSL-dating of aeolian sediments did not give an answer regarding the exact time of the studied Finow soils' fossilization. However, considering their location, climate change and the transformation of plant cover in the Late Glacial, it can be assumed that the activation of aeolian processes leading to soil process interruption occurred during the cold periods of the Late Glacial, mainly in the Older and the Younger Dryas.

4.2. Evidence of pedogenic processes in content of different Fe forms and mineral composition of the clay fraction of Finow soils

Mineralogical analyses of clay fractions from fossil Bwb horizons showed the predominance of dioctahedral clays. The most interesting phase in the context of genesis of the studied soils was dioctahedral vermiculite, which was present in the studied Bwb horizons (Fig. 4). That clay mineral forms in soils and weathering environments mainly at the expense of dioctahedral mica, for example, muscovite (Bain et al., 1990; Churchman, 1980; Douglas, 1989; Skiba, 2007; Skiba, 2013; Skiba et al., 2018; Yin et al., 2013; Yin et al., 2018; Yin et al., 2017). Dioctahedral vermiculite commonly occurs in soils and fresh sediments of cold and temperate climates (April et al., 1986; Bonifacio et al., 2009; Douglas, 1989). However, vermiculite rarely occurs in unweathered glacial deposits, where illite, kaolinite, chlorite, and smectite are the predominant phases (Długosz et al., 2009; Murray and Leininger, 1955; Willman et al., 1963). Therefore, the occurrence of dioctahedral vermiculite in the studied Bwb horizons indicated the effect of pedogenic processes.

The observed increase of Fe_t and Al_t contents in Bo and Bwb horizons in relation to the other sections of soil profiles underlines the trend toward iron and clay accumulation, especially in all B horizons (e.g. Jankowski, 2012). The higher content of Al_t in Bwb horizons proves indirectly about the enrichment in clay minerals which contain Al (e.g., diocahedral vemiculite). On the basis of the collected results it can be concluded that enrichment of Finow soils in Al results from enhancement in dioctahedral clay minerals. Free iron oxides (Fe_d) could either be a product of parent material weathering or come from groundwater and crystallize on the ice-soil boundary. This form is concentrated mainly at the surface soil horizons. Therefore, increased content of Fe_d and Fe_o in Bwb horizons can be linked to the initiation of the soil-forming process before burying. Values of weathering (Fe_d/Fe_t) ratio (Schwertmann, 1964), as well as Fe_o/Fe_d ratio, were low, which confirmed poor weathering of mineral substrates and low activity of iron oxides. However, these values were higher compared to neighbouring soil horizons (above and below Finow soil). Comparable relationships were found by Jankowski (2012).

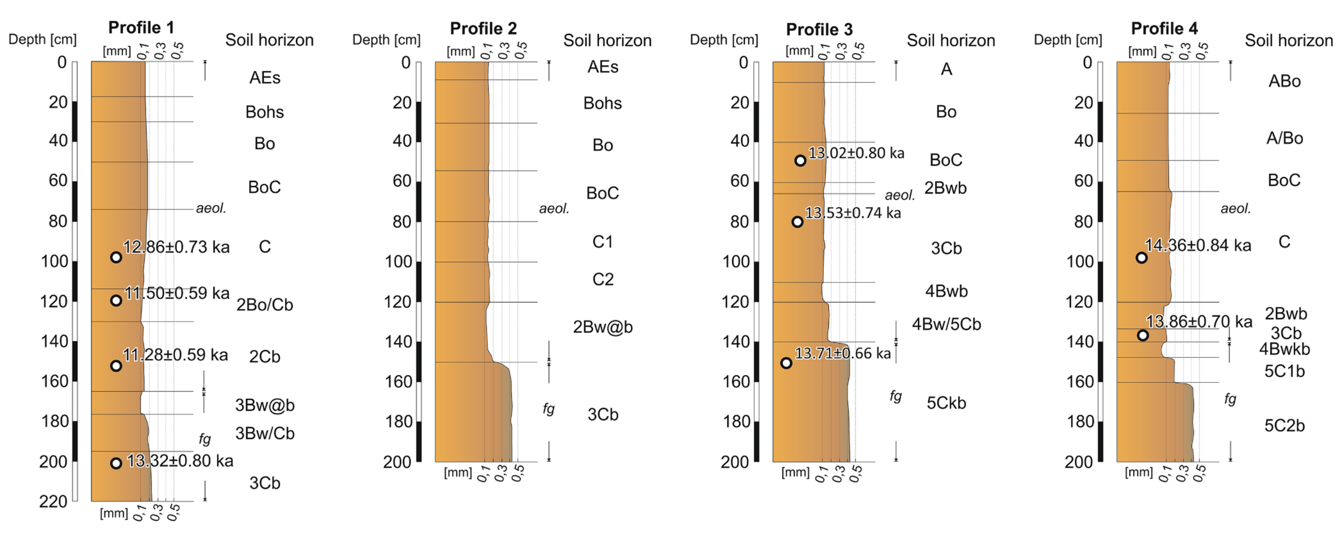

Fig. 5. Mean grain size and origin of deposits of the profiles.

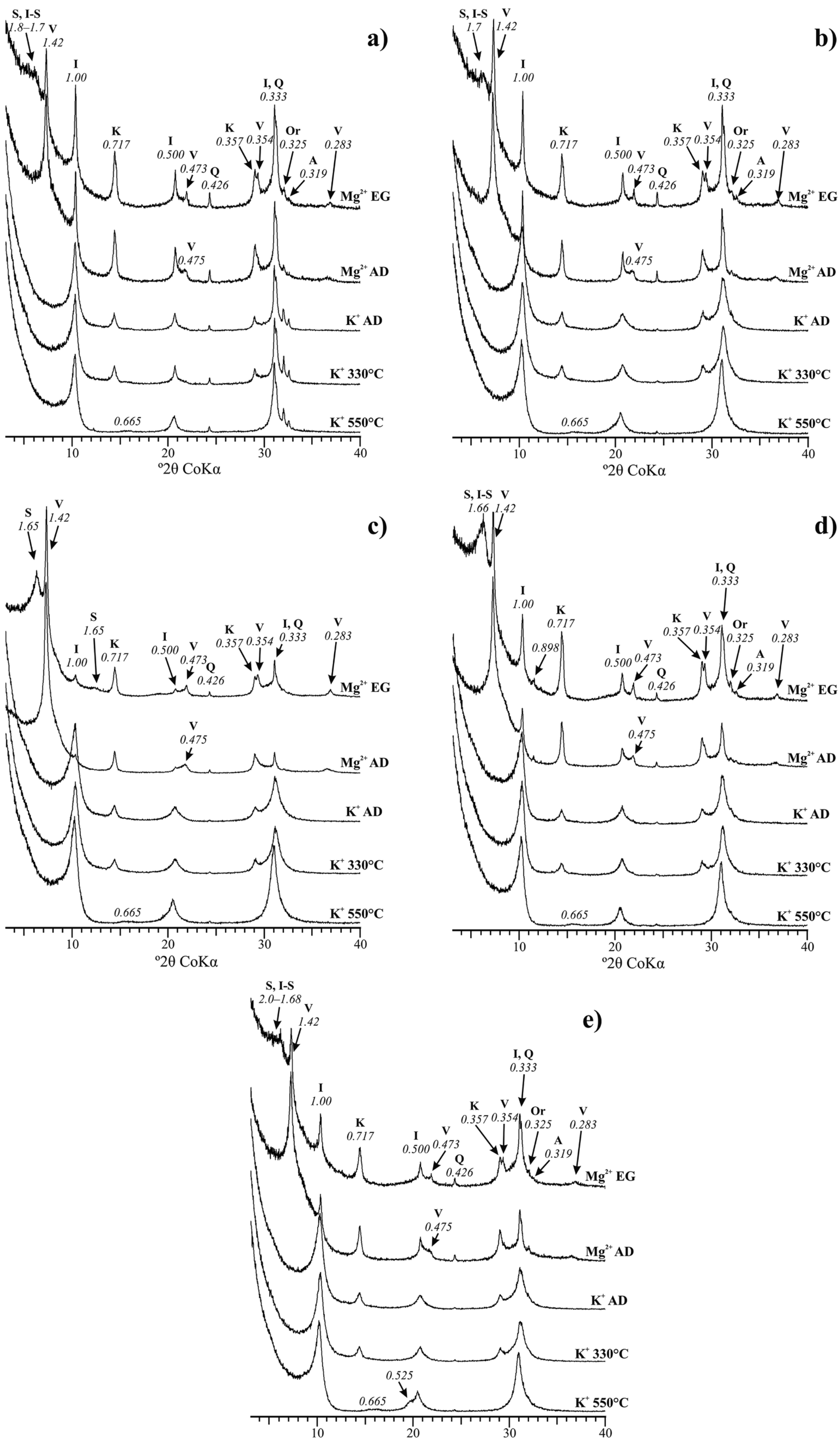

Fig. 6. XRD patterns of oriented mounts of clay fractions from studied soils. (a)—3Bw@b horizon (163–177 cm), profile 1; (b)—2Bw@b horizon (120–150 cm), profile 2; (c)—4Bwb horizon (110–120 cm), profile 3; (d)—4Bwkb horizon (140–148 cm), profile 4; (e)—2Bwb horizon (120–132 cm), profile 4. Mineral symbols: A—albite; I—illite; I-S—illite-smectite; K—kaolinite; Or—orthoclase; Q—quartz; S—smectite; V—vermiculite. The d values (in italics) are in nm.

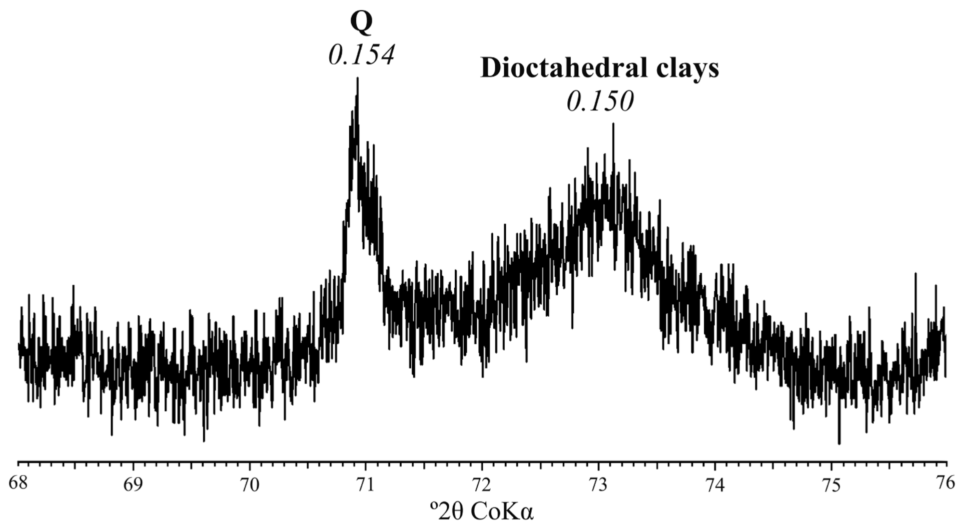

Fig. 7. Selected XRD pattern of random powder mount of clay fraction from 4Bwb horizon (110–120 cm), profile 3. Mineral symbols: Q—quartz. The d values (in italics) are in nm.

4.3. Similarities and differences of Finow soil characteristics in Europe and Asia

Dune systems exhibit successional development of soil cover strongly conditioned by vegetation cover and general environmental conditions, e.g. parent material and climate (Jones et al., 2008). Considering the relatively young age of the aeolian sediments it may be assumed that they represent the earliest stage of soil development after surface stabilization by plant cover. In view of physical and chemical properties (sandy texture, low content of nutrients, etc.) and given that there were no traces of other prevailing soil-forming processes, soils developed at the surface of aeolian sediments were classified according to the WRB classification system (IUSS Working Group WRB, 2015) as Dystric Brunic Arenosols (Aeolic, Protospodic) and Dystric Brunic Arenosols (Aeolic). With Podzols, this soil type is typical for inland dunes (Jankowski, 2010; Sewerniak and Jankowski, 2017). Paleosols found in the study area were classified as Eutric Brunic Arenosols (Relictiturbic) (profile 1 and 2), and Eutric Cambisols (Loamic) (profile 3 and 4, in view of relatively high content of silt and clay and the presence of cryogenic features in profile) (Figs. 2 and 3). The Finow soils are usually classified as loamy sand Brunic Arenosols (Hilgers, 2007; Jankowski, 2012; Kaiser et al., 2009; Konstantinov et al., 2019). However, the first recorded Finow soil was described as 5–15 cm thick Dystric Cambisol over glaciofluvial deposits and devoid of humus horizon (Schlaak, 1993). The studied profiles are characterized by low P, K, Ca and Mg content, which is typical for nutrient deficient sandy material (e.g. Kruczkowska et al., 2017). Finow soils reported in previous studies (Jankowski, 2012; Kaiser et al., 2009; Konstantinov et al., 2019; Küster and Preusser, 2009) have similar physical and chemical properties in comparison to Lake Gościąż profiles, however, characteristics of grain-size distribution in Bwb horizons of the investigated profiles were distinct from other Finow soil stands. According to description of Finow soils by Schlaak (1993), Bwb horizons should be characterized by an increase in the silt and clay content when compared to deposits lying below and above Bwb horizons. The latest studies on Finow soils (Jankowski, 2012; Kaiser et al., 2009; Küster et al., 2014; Küster and Preusser, 2009) indicated that the particle-size distribution shows the dominance of sand fraction in all soil horizons, which ranged from 83% to 98%. In the previously described Finow soil profiles, silt content varied between 1% and 16% and clay content between 1% and 5%. Fossil soils developed in the direct vicinity of Lake Gościąż are characterized by a higher content of fine fractions – up to 41.1% of silt and 14.0% of clay. Higher content of coarser fractions can be partially correlated with periglacial processes (e.g., material mixing during formation of ice wedges occurring in profile 1). Origin of illuvial lamellae observed below Bwb horizons is probably post-burial (Jankowski, 2012). Their horizontal stratification referred to the positions of fossil Bwb horizons. As Jankowski (2012) noticed, lamellae underlie some structural features of Finow soils and sediments, which are also confirmed in the studied soils. According to the NRCS-SSURGO Official Soil Descriptions the lamellae most commonly have a loamy sand, loamy fine sand, or sandy loam texture and mean maximum thickness of 22 mm (Bockheim and Hartemink, 2013). They are commonly formed in sandy materials (Berg, 1984; Schaetzl, 2001) and are often associated with iron oxides (Bockheim and Hartemink, 2013). Results obtained by Obear et al. (2017) also indicate a lower clay content, ranging from 0.10% to 3.8%. In view of these results, the concept of linking the Finow soils origin with lamellae formation seems to be debatable. However, according to Berg (1984) and Holliday and Rawling (2006), in chronosequences developed in dune sands, thickness of lamellae increases with time, which certainly is not a proof of the final conversion into Finow soils.

In Western and Central Europe, the presence of Finow soils with similar properties indicates indirectly analogical environmental conditions on the whole foreland of the ice sheet. Favourable conditions for the formation of Finow soils should have occurred at certain intervals, interrupted by periods of intensified accumulation of sand cover (Kaiser et al., 2009). Distinct transitions between Finow soils and cover deposits indicate an increased intensity of weathering as a result of periglacial conditions. The presence of ice wedges and cryoturbations (Fig. 2) in the studied profiles is a testimony to the overlapping of periglacial conditions (e.g. frost action) on soil-forming processes. It should be noted that cryoturbations are visible within Finow soil profiles, which indicates that these soils probably had to develop on the land surface and not after its fossilization. There are no signs of cryoturbation in sediments covering Finow soils.

High $CaCO_3$ content in the bottom part of profile 4 could suggest the existence of a small water pool directly after fluvioglacial accumulation of carbonate-rich organic remains. However, the results of analysis of macrofossils showed that there is a lack of fossils in tested samples. It can be treated as an indicator of the periodic nature of this water reservoir and adverse conditions for the living organisms development, e.g. very cold climate. Therefore, it should be assumed that carbonates accumulated in this sediment were related to the precipitation of cryochemical carbonates from mineralized waters, which is also confirmed by the research conducted in other areas (Bukowska-Jania, 2003; Słowiński et al., 2015; van Loon et al., 2012). This form of $CaCO_3$ was crystallized under periglacial conditions and was the most susceptible to re-dissolution and migration.

5. Conclusions

The paleosol profiles were identified as Finow soils and are characterized by physical and chemical features similar to other examples of this type of soils with differences in soil texture. In the studied Bwb horizons dioctahedral vermiculite was found, which is typically a pedogenic clay mineral. The formation of vermiculite indicated formation of Bwb horizons likely due to soil-forming processes. Pedogenic origin of Bwb horizons was further indicated by the increased contents of various forms of iron and aluminium within the studied horizons in comparison with neighbouring sediments. These soils were covered with aeolian sediments during cold climatic phases (stadials) as indicated by the presence of ice wedges and cryoturbations. OSL dating of aeolian sediments below and above the Finow soil did not provide unequivocal results but most ages suggest a pre-Allerød formation. However, since one Younger Dryas age has been obtained, soil formation in some locations during the Allerød cannot be excluded. In other regions with Finow soil occurrences like Germany, Northern Poland and Western Siberia, most ages suggested soil formation in the Bølling/Allerød and coverage during colder periods of the Late Glacial (the Older Dryas and the Younger Dryas). Further studies are needed to finally resolve whether the older, pre-Allerød ages were related to dating uncertainties or if they reflect multiple soil formation periods in the different Late Glacial interstadials.

Acknowledgements

This study is a contribution to scientific project financed by the National Science Centre, Poland – No. UMO-2015/19/B/ST10/03039.

References

Aichner, B., et al., 2018. Leaf wax n-alkane distributions record ecological changes during the Younger Dryas at Trzechowskie paleolake (northern Poland) without temporal delay. Clim. Past 14, 1607–1624.
Aitken, M.J., 1998. An Introduction to Optical Dating. Oxford University Press, Oxford, The Dating of Quaternary Sediments by the Use of Photon-stimulated Luminescence.
April, R.H., Hluchy, M.M., Newton, R.M., 1986. The nature of vermiculite in adirondack soils and till. Clays Clay Miner. 34, 549–556.
Arbeitskreis Standortskartierung, 1996. Forstliche Standortsaufnahme. 5Auflage. IHW-Verlag Eching bei München.
Arbogast, A.F., Schaetzl, R.J., Hupy, J.P., Hansen, E.C., 2004. The Holland Paleosol: an informal pedostratigraphic unit in the coastal dunes of southeastern Lake Michigan. Can. J. Earth Sci. 41, 1385–1400.
Bain, D.C., Mellor, A., Wilson, M.J., 1990. Nature and origin of an aluminous vermiculitic weathering product in acid soils from upland catchments in Scotland. Clay Miner. 25, 467–475.
Bartczak, A., et al., 2019. Ecohydrological changes and resilience of a shallow lake ecosystem under intense human pressure and recent. Clim. Change Water, 11.
Berg, R.C., 1984. The origin and early genesis of clay bands in youthful sandy soils along lake Michigan, U.S.A. Geoderma 32, 45–62.
Birks, H.H., 2007. Plant macrofossil introduction. In: Elias, S.A. (Ed.), Encyclopedia of Quaternary Science. Elsevier, Amsterdam, pp. 2266–2288.
BK5, 2005. Bodenkartieranleitung, E. Schweizerbartische Verlagsbuchhandlung, Stuttgart, 438.
Blott, S.J., Pye, K., 2001. GRADISTAT: a grain size distribution and statistics package for the analysis of unconsolidated sediments. Earth Surf. Proc. Land. 26, 1237–1248.
Błaszkiewicz, M., 2011. Timing of the final disappearance of permafrost in the central European Lowland, as reconstructed from the evolution of lakes in N Poland. Geol. Quart. 55, 361–374.
Błaszkiewicz, M., Gruszka, B., 2005. Development and infill of Vistulian glacial Lake Gniew (N Poland): a sedimentological analysis. Geol. Quart. 49, 449–462.
Błaszkiewicz, M., et al., 2015. Climatic and morphological controls on diachronous postglacial lake and river valley evolution in the area of Last Glaciation, northern Poland. Quat. Sci. Rev. 109, 13–27.
Bockheim, J.G., Hartemink, A.E., 2013. Classification and distribution of soils with lamellae in the USA. Geoderma 206, 92–100.
Bonifacio, E., Falsone, G., Simonov, G., Sokolova, T., Tolpeshta, I., 2009. Pedogenic processes and clay transformations in bisequal soils of the Southern Taiga zone. Geoderma 149, 66–75.
Bøtter-Jensen, L., Bulur, E., Duller, G.A.T., Murray, A.S., 2000. Advances in luminescence instrument systems. Radiat. Meas. 32, 523–528.
Brauer, A., Endres, C., Negendank, J.F.W., 1999. Lateglacial calendar year chronology based on annually laminated sediments from Lake Meerfelder Maar, Germany. Quat. Int. 61, 17–25.
Brauer, A., Günter, C., Johnsen, S.J., Negendank, J.F.W., 2000. Land-ice teleconnections of cold climatic periods during the last Glacial/Interglacial transition. Clim. Dyn. 16, 229–239.
Bukowska-Jania, E., 2003. The role of glacier system in the migration of calcium carbonate in the natural environment – with particular reference to Svalbard and the late – glacial areas in NW Poland (in Polish), Prace Naukowe. Wydawnictwo Uniwersytetu Śląskiego, Katowice, pp. 247.
Churchman, G.J., 1980. Clay minerals formed from micas and chlorites in some New Zealand soils. Clay Miner. 15, 59–76.
Churski, Z., 1998. Location of Lake Gościąż and the Gostynińskie Lake District. In: Ralska-Jasiewiczowa, M., Goslar, T., Madeyska, T., Starkel, L. (Eds.), Lake Gościąż, Central Poland. A monographic study, Part I. W. Szafer Institute of Botany, Polish Academy of Sciences, Krakow, Poland, pp. 3.
Długosz, J., Orzechowski, M., Kobierski, M., Smólczyński, S., Zamorski, R., 2009. Clay minerals from Weichselian glaciolimnic sediments of the Sępopolska Plain (NE Poland). Geol. Carpath. 60, 263–267.
Douglas, L.A., 1989. Vermiculites. In: Dixon, J.B., Weed, S.B. (Eds.), Minerals in Soil Environments. Soil Science Society of America, Madison, Wisconsin, USA, pp. 635–668.
Duller, G.A.T., 2008. Single-grain optical dating of Quaternary sediments: why aliquot size matters in luminescence dating. Boreas 37, 589–612.
FAO, 2006. Guidelines for soil description. 4th ed. ftp://ftp.fao.org/agl/agll/docs/guidel_soil_descr.pdf, Rome.
Feurdean, A., et al., 2014. Climate variability and associated vegetation response throughout Central and Eastern Europe (CEE) between 60 and 8 ka. Quat. Sci. Rev. 106, 206–224.
Folk, R.L., Ward, W., 1957. Brazos River bar: a study in the significance of grain size parameters. J. Sediment. Petrol. 3–26.
Galbraith, R.F., Roberts, R.G., Laslett, G.M., Yoshida, H., Olley, J.M., 1999. Optical dating of single and multiple grains of quartz from jinmium rock shelter, northern australia: part i, experimental design and statistical models*. Archaeometry 41, 339–364.
Guerin, G., Mercier, N., Adamiec, G., 2011. Dose-rate conversion factors: update. Ancient TL 5–8.
Hilgers, A., 2007. The Chronology of Late Glacial and Holocene Dune Development in the Northern Central European Lowland Reconstructed by Optically Stimulated Luminescence. (OSL) Dating, University of Cologne, pp. 353 pp..
Bukowska-Jania, E., 2003. The role of glacier system in the migration of calcium carbonate in the natural environment – with particular reference to Svalbard and the late – glacial areas in NW Poland (in Polish), Prace Naukowe. Wydawnictwo Uniwersytetu Śląskiego, Katowice, pp. 247.
Holliday, V.T., Rawling, J.E., 2006. Soil-geomorphic relations of lamellae in eolian sand on the High Plains of Texas and New Mexico. Geoderma 131, 154–180.
Jackson, M.L., 1975. Soil Chemical Analysis – Advanced Course. Madison, Wisconsin, USA.
Jankowski, M., 2002. Buried soils in dunes of the Toruń Basin. In: Manikowska, B., Konecka- Betley, K., Bednarek, R. (Eds.), Paleopedology Problems in Poland. Towarzystwo Naukowe, Łódź, Łódzkie, pp. 233–252.
Jankowski, M., 2010. Some aspects of site conditions of heathlands in the Toruń Basin. Ecological Questions 149–156.
Jankowski, M., 2012. Lateglacial soil paleocatena in inland-dune area of the Toruń Basin, Northern Poland. Quat. Int. 265, 116–125.
Jones, M.L.M., Sowerby, A., Williams, D.L., Jones, R.E., 2008. Factors controlling soil development in sand dunes: evidence from a coastal dune soil chronosequence. Plant Soil 307, 219–234.
Kaiser, K., et al., 2009. Palaeopedological marker horizons in northern central Europe: characteristics of Lateglacial Usselo and Finow soils. Boreas 38, 591–609.
Kalińska-Nartiša, E., Nartišs, M., Thiel, C., Buylaert, J.P., Murray, A.S., 2015. Late-glacial to Holocene aeolian deposition in northeastern Europe – the timing of sedimentation at the Iisaku site (NE Estonia). Quat. Int. 357, 70–81.
Kasse, C., 2002. Sandy aeolian deposits and environments and their relation to climate during the Last Glacial Maximum and Lateglacial in northwest and central Europe. Prog. Phys. Geogr. 26, 507–532.
Kępczyński, K., Noryśkiewicz, A., 1998. Vegetation of the Gostynińskie Lake Dystrict. In: Ralska-Jasiewiczowa, M., Goslar, T., Madeyska, E., Starkel, L. (Eds.), Lake Gościąż, Central Poland, a Monographic Study Part I. Szafer Institute of Botany Polish Academy of Sciences, Kraków, Poland, pp. 3.
Kolstrup, E., 1980. Climate and stratigraphy in northwestern Europe between 30,000 B.P. and 13,000 B.P., with special reference to The Netherlands. Rijks Geologische Dienst, pp. 181–253.
Kondracki, J., 2001. Geografia regionalna Polski. Wydawnictwo Naukowe PWN, Warszawa.
Konecka-Betley, K., 1974. Late-Pleistocenik and Holocenik fossil soils and relict soils in the vicinity of Otwock (Późnoplejstoceńskie i holoceńskie gleby kopalne i reliktowe okolic Otwocka). Roczniki Gleboznawcze - Soil Sci. Annual 25, 101–118.
Konecka-Betley, K., 1981. Development of the soil-forming processes of late Pleistocene and Holocene in dunes of the environs of Warsaw. Roczniki Gleboznawcze – Soil Sci. Annual 32, 151–160.
Konecka-Betley, K., 1982. Fossil and relict soils in dunes of the Warsaw environs (Gleby kopalne i reliktowe wydm okolic Warszawy). Roczniki Gleboznawcze – Soil Sci. Annual 33, 81–112.
Konecka-Betley, K., 1991. Late Vistulian and Holocene fossil soils developed from aeolian and alluvial sediments of the Warsaw Basin. Zeitschrift für Geomorphologie 90,

99–105.
Konstantinov, A. et al., 2019. First Findings of Buried Late-Glacial Paleosols within the Dune Fields of the Tomsk Priobye Region (SE Western Siberia, Russia). Geosciences, 9.
Koster, E.A., 1988. Ancient and modern cold-climate aeolian sand deposition: a review. J. Quat. Sci. 3, 69–83.
Kozarski, S., Nowaczyk, B., 1991. Lithofacies variation and chronostratigraphy of Late Vistualian and Holocene phenomena in northwestern Poland. Zeitschrift für Geomorphologie 90, 107–122.
Krajewski, K., Balwierz, Z., 1984. Stanowisko Bøllingu w osadach wydmowych schyłku Vistulianu w Roślu Nowym k/Dąbia. Acta Geogr. Lodz. 50, 93–112.
Kruczkowska, B., Jonczak, J., Gadziszewska, J., 2017. Characteristics of permafrost-affected soil in a cliff in the central part of the Polish Baltic coastal zone. J. Soils Sediments 17, 960–973.
Küster, M., Fülling, A., Kaiser, K., Ulrich, J., 2014. Aeolian sands and buried soils in the Mecklenburg Lake District, NE Germany: holocene land-use history and pedo-geomorphic response. Geomorphology 211, 64–76.
Küster, M., Preusser, F., 2009. Late Glacial and Holocene aeolian sands and soil formation from the Pomeranian outwash plain (Mecklenburg, NE-Germany). Quater. Sci. J. 58, 156–163.
Litt, T., et al., 2001. Correlation and synchronisation of Lateglacial continental sequences in northern central Europe based on annually laminated lacustrine sediments. Quat. Sci. Rev. 20, 1233–1249.
Litt, T., Stebich, M., 1999. Bio- and chronostratigraphy of the lateglacial in the Eifel region, Germany. Quat. Int. 61, 5–16.
Manikowska, B., 1970. Późnoplejstoceńskie gleby kopalne w wydmie koło Annopola nad Wisłą. Acta Geogr. Lodz. 327–336.
Manikowska, B., 1982. Gleby kopalne w wydmach Polski środkowej (Fossil soils in dunes of central Poland). Roczniki Gleboznawcze-Soil Sci. Annual 33, 119–133.
Manikowska, B., 1991. Vistulian and Holocene aeolian activity, pedostratygraphy and relief evolution in Central Poland. Zeitschrift für Geomorphologie 90, 131–141.
Mehra, O.P., Jackson, M.L., 1960. Iron oxide removal from soils and clays by dithionite-citrate system buffered with sodium bicarbonate. Clays and Clay Minerals, Proceedings of 7th National Conference. Pergamon Press, Oxford, UK, pp. 317–327.
Murray, A.S., Wintle, A.G., 2000. Luminescence dating of quartz using an improved single-aliquot regenerative-dose protocol. Radiat. Meas. 32, 57–73.
Murray, H.H., Leininger, R.K., 1955. Effect of weathering on clay minerals. Clays Clay Miner. 4, 340–347.
Obear, G.R., Pedersen, M., Kreuser, W.C., 2017. Genesis of clay lamellae in golf course soils of Mississippi, USA. CATENA 150, 62–70.
Płóciennik, M., Self, A., Birks, H.J.B., Brooks, S.J., 2011. Chironomidae (Insecta: Diptera) succession in Żabieniec bog and its palaeo-lake (central Poland) through the Late Weichselian and Holocene. Palaeogeogr. Palaeoclimatol. Palaeoecol. 307, 150–167.
Prescott, J.R., Stephan, L.G., 1982. The contribution of cosmic radiation to the environmental dose for thermoluminescence dating. TLS II-1. Latitude, altitude and depth dependencies, 16-25.
Polskie Towarzystwo Gleboznawcze, 2009. Klasyfikacja uziarnienia gleb i utworów mineralnych – PTG 2008 (Particle size distribution and textural classes of soils and mineral materials - classification of Polish Society of Soil Science 2008). Roczniki Gleboznawcze – Soil Science Annual, 60(2): 5–16.
Rach, O., Brauer, A., Wilkes, H., Sachse, D., 2014. Delayed hydrological response to Greenland cooling at the onset of the Younger Dryas in western Europe. Nat. Geosci. 7, 109–112.
Ralska-Jasiewiczowa, M., Goslar, T., Madeyska, T., Starkel, L., 1998. Lake Gosciąż central Poland, A monographic study part 1.
Rosenzweig, R., Porat, N., 2015. Evaluation of soil-moisture content for OSL dating using an infiltration model. Ancient TL, 10–14.
Rychel, J., Woronko, B., Błaszkiewicz, M., Karasiewicz, T., 2018. Aeolian processes records within the last glacial limit areas based on the Płock basin case (Central Poland). Bull. Geol. Soc. Finland 90, 55–69.
Sandgren, P., Thompson, R., 1990. Mineral magnetic characteristics of podzolic soils developed on sand dunes in the Lake Gosciaz catchment, central Poland. Phys. Earth Planet. Inter. 60, 297–313.
Schaetzl, R.J., 2001. Morphologic evidence of lamellae forming directly from thin, clayey bedding planes in a dune. Geoderma 99, 51–63.
Schlaak, N., 1993. Studie zur Landschaftsgenese im Raum Nordbarnim und Eberswalder Urstromtal. Berliner Geographische Arbeiten.
Schlaak, N., Kowalski, S., 2015. Finowboden – ważny horyzont stratygraficzny późnego glacjału. In: Kordowski, J., Lamparski, P., Lisicki, S., Roman, M. (Eds.), XXII konferencja naukowo-szkoleniowa. Plejstocen Kotliny Płockiej oraz Postglacjalna transformacja jej rzeźby. Stratygrafia plejstocenu Polski, Gołaszewo, pp. 98–99 (in Polish).
Schwertmann, U., 1964. Differenzierung der Eisenoxide des Bodens durch Extraktion mit Ammoniumoxalat e Lösung. Zeitschrift für Pflanzenernährung, Düngung, Bodenkunde, 105, 194–202.
Sewerniak, P., Jankowski, M., 2017. Topographically-controlled site conditions drive vegetation pattern on inland dunes in Poland. Acta Oecologica 82, 52–60.
Skiba, M., 2007. Clay mineral formation during podzolization in an alpine environment of the Tatra Mountains, Poland. Clays Clay Miner. 55, 618–634.
Skiba, M., 2013. Evolution of dioctahedral vermiculite in geological environments – an experimental approach. Clays Clay Miner. 61, 290–302.
Skiba, M., Skiba, S., Derkowski, A., Maj-Szeliga, K., Dziubińska, B., 2018. Formation of NH4-illite-like phase at the expense of dioctahedral vermiculite in soil and diagenetic environments – an experimental approach. Clays Clay Miner. 66, 74–85.
Słowiński, M., et al., 2015. The role of melting dead ice on landscape transformation in the early Holocene in Tuchola Pinewoods, North Poland. Quat. Int. 388, 64–75.
Słowiński, M., et al., 2018. Cascading effects between climate, vegetation, and macroinvertebrate fauna in 14,000-year palaeoecological investigations of a shallow lake in eastern Poland. Ecol. Ind. 85, 329–341.
Słowiński, M., et al., 2017. Differential proxy responses to late Allerød and early Younger Dryas climatic change recorded in varved sediments of the Trzechowskie palaeolake in Northern Poland. Quat. Sci. Rev. 158, 94–106.
USDA, 1993. Soil Survey Division Staff. Soil Survey Manual. Soil Conservation Service. 18. http://www.nrcs.usda.gov/wps/portal/nrcs/detail/soils/ref/?cid=nrcs142p2_054262. U.S. Department of Agriculture Handbook.
van Loon, A.J., Błaszkiewicz, M., Degorski, M., 2012. The role of permafrost in shaping the Late Glacial relief of northern Poland. Geol. Mijnbouw 91, 223–231.
van Reeuwijk, L.P., 2002. Procedures for soil analysis, sixth ed. ISRiC, FAO, Wageningen.
Vandenberghe, D.A.G., Derese, C., Kasse, C., Van den haute, P., 2013. Late Weichselian (fluvio-)aeolian sediments and Holocene drift-sands of the classic type locality in Twente (E Netherlands): a high-resolution dating study using optically stimulated luminescence. Quat. Sci. Rev. 68, 96–113.
Wicik, B., 1998. Soils in the vicinity of the Na Jazach Lakes. In: Ralska-Jasiewiczowa, M., Goslar, T., Madeyska, T., Starkel, L. (Eds.), Lake Gościąż, Central Poland. A monographic study, Part I. W. Szafer Institute of Botany, Polish Academy of Sciences, Krakow, Poland, pp. 29.
Willman, H.B., Glass, H.D., Frye, J.C., 1963. Mineralogy of glacial tills and their weathering profiles in Illinois. Part I. Glacial Tills. . Illinois State Geological Survey.
Woś, A., 1999. Climate of Poland. Wydawnictwo Naukowe PWN (in Polish), Warszawa, pp. 302.
Wójcik, G., Przybylak, R., 1998. Presend-day climatic conditions of the Lake Gościąż region. In: Ralska-Jasiewiczowa, M., Goslar, T., Madeyska, T., Starkel, L. (Eds.), Lake Gościąż, Central Poland. A monographic study, Part I. W. Szafer Institute of Botany, Polish Academy of Sciences, Krakow, Poland, pp. 4.
IUSS Working Group WRB, 2015. World Reference Base for Soil Resources 2014, update 2015. International soil classification system for naming soils and creating legends for soil maps. World Soil Resources Reports No. 106. FAO, Rome. http://www.fao.org/3/i3794en/I3794en.pdf.
Yin, K., et al., 2013. Hydroxy-interlayered vermiculite genesis in Jiujiang late-Pleistocene red earth sediments and significance to climate. Appl. Clay Sci. 74, 20–27.
Yin, K., Hong, H., Churchman, G.J., Li, Z., Fang, Q., 2018. Mixed-layer illite-vermiculite as a paleoclimatic indicator in the Pleistocene red soil sediments in Jiujiang, southern China. Palaeogeogr. Palaeoclimatol. Palaeoecol. 510, 140–151.
Yin, K., Hong, H., Pan, Y., Liu, Z., 2017. Mineralogy and genesis of mixed-layer illite-vermiculite in the homogeneous red soil and the net-like red soil of Xuancheng China. Appl. Ecol. Env. Res. 15, 675–686.
Zawiska, I., et al., 2015. The response of a shallow lake and its catchment to Late Glacial climate changes—a case study from eastern Poland. Catena 126, 1–10.
Zawisza, E., et al., 2019. Dystrophication of lake Suchar IV (NE Poland): an alternative way of lake development. Limnetica 38, 391–416.
Zeeberg, J., 1998. The European sand belt in eastern Europe - and comparison of Late Glacial dune orientation with GCM simulation results. Boreas 27, 127–139.